DRAG OF SPHERES IN DILUTE AQUEOUS SOLUTIONS OF POLY (ETHYLENE OXIDE) WITHIN THE REGION OF THE CRITICAL REYNOLDS NUMBER

JOHN HENRY CHENARD

DRAG OF SPHERES IN DILUTE AQUEOUS SOLUTIONS OF POLY(ETHYLENE OXIDE) WITHIN THE REGION OF THE CRITICAL REYNOLDS NUMBER

by

John Henry Chenard
Lieutenant, United States Navy
B.S., U.S. Naval Academy, 1960

Submitted in partial fulfillment of the
requirements for the degree of

MASTER OF SCIENCE IN PHYSICS

from the

NAVAL POSTGRADUATE SCHOOL
December 1967

ABSTRACT

The drag reducing effect of poly(ethylene oxide) additives on blunt bodies in water was investigated by examining the behavior of a sphere in both subcritical and supercritical Reynolds number regions. Drop tests were conducted in water and in concentrations of poly(ethylene oxide) WSR 301 ranging in concentration from 50 wppm to 1000 wppm. Reduction in drag was noted for all concentrations in the Reynolds number range of 4×10^4 to 3.5×10^5. A critical Reynolds number of 4.5×10^5 was observed for dilute solutions (50 and 100 wppm), while more concentrated solutions exhibited a uniformly decreasing drag. These results are explained by examining the interaction of profile and friction drag, together with the effects of polymer additives upon wake diameter size.

TABLE OF CONTENTS

LIST OF ILLUSTRATIONS

LIST OF TABLES

SYMBOLS AND ABBREVIATIONS

A	Maximum cross-sectional area
B	Buoyant force
C	Measured coefficient of drag
$\underline{C}$	Time dependent coefficient of drag
C_D	Terminal drag coefficient
d	Sphere diameter in centimeters
D	Drag force
g	Gravitational acceleration
h	Actual fall distance
K	Virtual mass coefficient
m	Mass of fluid displaced by sphere
Re	Reynolds number based on viscosity of water
s	Vertical position (cm) from point of release
$\dot{s}$	Velocity: ds/dt
$\ddot{s}$	Acceleration: d^2s/d^2t
T	String tension
v	Terminal velocity
V	Volume of sphere
w	Counterbalance weight
α	Ratio of instantaneous velocity to terminal velocity
ρ'	Effective density of sphere
ρ	Density of water
μ	Dynamic viscosity of water

1. Introduction

A major objective of hydrodynamicists and ship designers is to increase the speed of ships at the least possible expenditure of money and weight. At present, twenty knots is considered to be a very good speed for merchant ships. For increases in speed in excess of twenty knots, it has been proven that the increased propulsive power requirements are economically infeasible. For example, in order to double the top speed of a typical merchant ship, it would be necessary to increase the propulsive power by a factor of about ten. Clearly, this is not the optimum way to achieve the increased speed objectives.

The hydrodynamic barrier preventing the achievement of this objective is drag resistance. For the purpose of analysis, drag resistance can be separated into two distinct components, which, for surface ships, are of approximately equal importance: wave-making resistance and viscous resistance.

There have been numerous attempts to effectively reduce viscous drag, the more successful of which are presented below:

Laminarization, which is an application of the laminar airfoil concept, decreases skin friction significantly. This technique is of little use for surface vessels since it requires a prohibitively high degree of hull smoothness in order to maintain laminar flow, and in addition, the sea surface is so turbulent that achievement of laminar flow would be difficult. However, when laminarization techniques are applied to submerged bodies, drag reduction is readily apparant, as evidenced by recent tests conducted by North American Aviation Corp., with negatively buoyant bodies.

Suction and blowing techniques are equally effective in decreasing skin friction, but infeasible to date due to machinery considerations and the fouling of intakes.

Hydrofoil vessels attempt to minimize the problem of skin friction and wake drag by lifting the hull clear of the water. Commercially built ships of this design have attained speeds in excess of

forty-five knots. However, there are definite cargo weight limitations which preclude widespread commercial application.

High polymer additives are a new approach to the problem of reducing drag. In spite of the fact that the mechanism is not completely understood, much experimental progress has been made in a short period of time. It has been determined that turbulent skin friction is greatly reduced in a high polymer solution.

Initial research of polymer solutions concerned the reduction of turbulent skin friction for flow in pipes and about rotating discs. For this type flow, fluid dynamic drag was greatly reduced by extremely low concentrations of polymer additives. The greatest drag reduction was achieved with polymers having the longest chain molecules, i.e. a very large length to diameter ratio.

In order to study separation drag, it is necessary to use blunt bodies. Since the sphere is the simplest of blunt bodies, it is the logical choice with which to start. In addition, for comparison purposes, the flow of a Newtonian fluid about a sphere has been extensively studied.

From previous research, it has been observed that polymer additives are effective in reducing both turbulent skin friction and separation drag, as can be seen in Table 2.1. The physical mechanism involved is not clearly understood, but is very possibly the same for both types of flow.

TABLE 2.1

Comparison of WSR 301 Drag Reduction

For Various Geometries

Type of Flow	Polymer Conc. (wppm)	% Drag Reduction
pipe	25	65
rotating disc	50	40
sphere	100	54

WSR 301, which is manufactured by Union Carbide, was the polymer selected for study since it produced the greatest drag reduction. It is a water soluble, non-corrosive, non-toxic polymer of ethylene oxide with a molecular weight of four million. Since it has many commercial applications, it is relatively inexpensive, presently costing less than one dollar per pound.

It is the purpose of this paper to investigate the effects of high polymers on separation dominated flows. In particular, investigation will be concentrated on the behavior of a blunt body in the critical Reynolds number region, since previous observations were conducted for subcritical Reynolds numbers.

2. Earlier Experiments with Spheres

The earliest extensive investigation of spheres in a high polymer solution was conducted by Ruszczycky [1] in 1965. He used spheres of diameters ranging from 0.375 in. to 1.0 in. in solution concentrations from 2500 wppm (0.25%) to 15000 wppm (1.5%). The maximum drag reduction attained was 26% in a 7500 wppm (0.75%) solution of WSR 301. From these results, the initial conclusion was that polymers are less effective for wake dominated flow than for turbulent pipe flow.

In 1966, Hayes [2] conducted a series of drag coefficient measurements using free falling metal spheres of diameters from 0.038 in. to 1.0 in. He investigated optimum concentrations and type of polymer for a range of water Reynolds numbers of 10^3 to 6×10^4 for four different grades of polymers. The concentration range investigated was from 10 wppm (0.001%) to 1000 wppm (0.1%). Hayes reported a maximum drag reduction of 54% in 100 wppm (0.01%) of WSR 301. In addition, he found that drag reduction occurs only for water Reynolds numbers greater than 10^4 and that the amount of drag reduction increases with Reynolds number, for Reynolds numbers less than critical.

In comparing the data of Hayes and Ruszczycky, it is readily apparent that Hayes reported a drag reduction that was twice as great as did Ruszczycky and at much lower concentrations. Thus there are two distinct regions of drag reduction with probably two different physical mechanisms existing.

In 1966, D.A. White [3] essentially duplicated the experiment of Hayes, using WSR 301 and spheres of diameters from 0.344 in. to 0.8 in. He achieved a maximum drag reduction of 45% in 75 wppm (0.0075%) solution of polyox and his conclusions substantiated the findings of Hayes.

Lang and Patrick [4], using spheres of diameters up to 2.5 in., investigated drag reduction for water Reynolds numbers up to 2×10^5. Where the data overlaps, their results are in close agreement with the findings of Hayes. For Reynolds numbers greater than 10^5 and

less than critical, they discovered that drag coefficients continue to decrease with increasing polymer concentration, at least up to 1000 wppm. In addition, dye streak photographs clearly show that the diameter of the wake is decreased by the addition of polymer when the Reynolds numbers are less than critical. For Reynolds numbers greater than critical, the wake diameter is increased, an indication that turbulent separation has been suppressed.

A. White [5], using a 7.75 in. sphere in a 60 wppm (0.006%) solution of WSR 301 verified the fact that addition of polymer moves the separation point forward when the Reynolds numbers are greater than critical.

3. Apparatus and Experimental Procedure

3.1 General. The objective of this research is to investigate the hydrodynamic behavior of spheres in polymer solutions by studying the drag coefficient. For a sphere of known diameter and with a predetermined polymer concentration, the measurement of drag force and terminal velocity permits the computation of a unique drag coefficient. By varying the terminal velocity and polymer concentration, a series of drag coefficients can be obtained, thus allowing for a systematic analysis of the polymer effects.

The experimental apparatus used in this research consisted of a sphere, tank, drop mechanism, and associated measuring and recording equipment.

3.2 Sphere. The test shape used in all phases of the experiment was a six inch hollow aluminum sphere, shown in Figs. 1 and 2. This sphere was machined by the Naval Postgraduate School machine shop. By utilizing a hollow shape, it was possible to employ ballast to produce various amounts of negative buoyancy. In addition, this arrangement makes possible the installation of internal instrumentation to investigate the boundary layer characteristics in polymer solutions.

The two halves of the sphere were fitted together by means of internal, partially threaded shafts, as shown in Fig. 2. In addition to facilitating machining procedures, this shaft provided a means of easy attachment of the internal ballast weights.

A watertight seal was attempted by fitting an O-ring in a groove between the two halves. When this did not prove entirely satisfactory, the two halves were re-machined to fit smoothly together. Dimethylpolysiloxane, a high kinematic viscosity (500,000 centistokes) lubricant was applied to mating surfaces, while Vinyline cement was used to seal the seam after the sphere was fitted together.

The empty sphere weighed 1110 gms. in air and, in water, had a positive buoyance of 745 gm. Two different ballast weights were used for the experiment. An 863 gm. brass weight provided for measurements

for the lower Reynolds number range of $3x10^4$ to $9x10^4$. A 3600 gm. lead ballast was used to obtain Reynolds numbers from $8x10^4$ to $5.8x10^5$.

3.3 Drop Tank. The tank design selected was a metal cylinder measuring six feet deep and three feet in diameter, with portholes in the side for visual observation of the falling sphere. Due to the dimensions of the tank, it was unnecessary to correct for wall effects. The tank interior was painted with two coats of red lead undercoating, followed by two coats of commercial swimming pool paint. As a result, negligible rusting occurred, except occasionally at weld beads and seams.

3.4 Mechanical System. A drive mechanism was the first consideration for a means of allowing the sphere to drop at a fixed rate. This procedure would have the advantage of being easily controlled and, in addition, would allow for precise control of velocity. One factor not recognized at the beginning was the need for an extremely steady drive due to the accuracy requirements of the drag force measurements.

The first drive mechanism attempted was the B&K strip recorder, Model #2305, with an external drive shaft attached. Since both paper speed and drive shaft speed were separately selectable, this versatile recorder allowed for a wide range of selectable velocities, which in this application, allowed for measurements as low as six centimeters per second. However, at low velocities, it was impossible to measure the correspondingly low drag forces. In addition, since the drive shaft had to hold the sphere in water prior to the drop, the plastic drive shaft gears inside the recorder had a tendency to strip.

The next drive mechanism tested was a 1/4 horsepower, variable speed electric motor. This machine was unable to provide a constant drive throughout the run, and, as a result, terminal velocity was never attained.

It was next decided to use the simple drop mechanism shown in Fig. 3. This mechanism allowed the velocity to be varied while still

permitting measurement of the drag force. In this system, the sphere was suspended beneath the water surface by means of a braided nylon line, which passed over a 9.25 cm. diameter free turning pulley, to a counter-balance and a quick release mechanism. This system proved to be successful and, with minor modifications, was used to obtain all data in this report. The nylon line was used in order to help dampen the vibrations which resulted from the sudden starting acceleration. Wire had earlier proved unsatisfactory due to a tendency to transmit oscillations, which in turn, caused tension readings to be difficult to analyze. In addition, tests showed that by passing the line around the pulley three times, additional vibrations were eliminated. To prevent the sphere from hitting the bottom of the tank, and also to preclude tension measuring instruments from being immersed in the tank, a safety line was attached to the strain gage support.

3.5 Instrumentation. As a means of obtaining displacement, and hence velocity, a five turn linear potentiometer was attached directly to the pulley shaft. The voltage output of the potentiometer was directly proportional to the distance traveled by the sphere. Velocity was varied by the addition of counterbalance weights. This procedure allowed for a wide range of velocities, all of which were easily reproducible.

Drag force measurements were obtained from the tension in the system, which varied with velocity. This tension was measured by a Statham UC-3 strain gage used in conjunction with the UR-5 Readout Meter.

The UC-3 strain gage is very sensitive to small forces, yet able to withstand large mechanical overloads. It has a force range of zero to sixty grams, which is easily extended by means of a variety of load cell adaptors. Instrument calibration instructions, as stated by the manufacturer, are minimal. First, adjust the UR-5 for 5/6 of full scale deflection according to instructions. Do not readjust after attaching the load cell adapter to the strain gage. Any attempt to

calibrate to read grams directly will result in a non-linearity of readout. In addition, "drift" of readings may possibly result after extended periods of use, which will necessitate recalibration.

3.6 Measurements. Velocity was determined from displacement versus time graphs which were plotted directly from potentiometer output. A typical graph is shown in Fig. 4. This output was calibrated by comparison with known distances.

Drag force on the sphere was obtained directly from tension readout of the UR-5, a plot of which is shown in Fig. 5. Due to the position of the strain gage in the system, friction of the pulley does not effect tension measurements. Calibration was accomplished by attaching known weights to the strain gage, and recording the results. In this way, time variations of readout linearity were verified at the same time.

At the higher Reynolds number range investigated (greater than 10^5), a comparison of tension readout with the corrected weight of the sphere in water revealed that friction force was relatively small and practically non-existent. Therefore, for this range of Reynolds numbers, the drag force was taken to be equal to the weight of the sphere in water minus the counterbalance weight.

4. Recording Instruments

Data was initially recorded on an eight channel tape recorder. This allowed all data to be taken during a single drop and stored for analysis at a later time. However, comparison of tape recorder output with direct readings indicated a small, yet important, difference of values. As a result, further use of the tape recorder was discontinued pending investigation of possible calibration errors.

Drag force data was plotted directly from the UR-5 Readout by means of a x-t plotter. Since only one, single pen plotter was available, it was possible to record only one parameter per drop.

An oscilloscope was used simultaneously with the x-t plotter in order to measure velocity. The oscilloscope had the advantage of a faster time base, which allowed for accurate determination of the higher velocities.

For the higher Reynolds number range investigated, the B&K Model #2305 recorder was used to record displacement versus time. In addition to the advantage of ease of use, the B&K recorder had paper speed range selectable up to 10 centimeters per second, a necessary feature for the high velocities investigated.

5. Formulation

5.1 General. The hydrodynamic drag characteristics of spheres, both in water and in polymer solutions, are clearly characterized by evaluating drag coefficients as a function of Reynolds number. For spheres, the drag coefficient is

$$C_D = \frac{\text{Drag Force}}{1/2\ \rho v^2\ A} \tag{1}$$

where $1/2\ \rho\ v^2$ is the dynamic pressure and A is the maximum cross-sectional area. In this equation, drag force and velocity are the experimentally measured quantities. This formula is applicable to both laminar and turbulent flow regions.

Reynolds number is defined as $Re = \frac{vd\rho}{\mu}$ (2)

where v is velocity, d is sphere diameter, ρ is fluid density, and μ is shear viscosity of the solution. In all cases, μ was taken to be equal to the viscosity of water, since viscometer measurements [6] have indicated that dilute polymer solutions of WSR 301 have a viscosity which is almost equal to that of water.

5.2 Analysis of velocity measurements. Evaluation of the initial high velocity results revealed the fact that terminal velocity was not being attained, a problem which was not present during the slower speed drops. The immediate consequences of using a velocity slower than terminal can be seen from equations (1) and (2). For a given drag force, the inaccurate, slower velocity produces a larger coefficient of drag, occurring at a lower than normal Reynolds number.

The fall distance required for a sphere to reach 0.99 terminal velocity was computed by means of a direct application of the integrated equation of motion for falling bodies, as derived by Lang and Patrick [4]. The only modification to this formula

$$S(.99) = \frac{1.96m(\rho'/\rho + K)}{1/2\ \rho A C_D} \tag{3}$$

is that the term ρ' must be considered to be the effective density of the sphere. It will be shown later that this effective density is a variable depending upon the counterbalance weight selected; and $\rho' = \frac{W+w}{gv}$, where W equals the weight of the sphere in air, w equals counterbalance weight, g is gravitational acceleration, and V equals sphere volume.

The results of applying Eq. 3 for W=5086 gm are presented in Table 5.1.

TABLE 5.1

Fall Distance Requirements

Counterbalance Wt.	Distance Required
0 gm.	10.4 feet
500	11.1
1000	12
3000	15

Since the only tank available for free fall drops was six feet in depth, it was necessary either to modify experimental procedure or to apply an acceleration correction to existing results, in order to investigate polymer behavior in the critical Reynolds number region.

The first method attempted was to use existing apparatus, and to initiate the drop one foot above the water surface. The results obtained were quite inconsistent due to the attached air bubble following the sphere in water. This bubble changed the configuration of the sphere to a streamlined body of revolution, thus invalidating all results.

It was therefore decided to conduct an analysis of displacement versus time plots, using the derivations of Lang and Patrick [4], as modified by Hayes [2], to arrive at an acceleration correction factor for C_D and Reynolds number.

The drop mechanism employed is essentially an Atwood's machine, with the sphere in water and the counterbalance weight in air. The following equations of motion are derived from free body diagrams of

the counterbalance and the sphere:

$$T - w = \frac{w}{g}\ddot{s} \tag{4}$$

and

$$W - B - T - D = \left(\frac{W}{g} + K\rho V\right)\ddot{s} \tag{5}$$

where T is tension in the string, w is the counterbalance weight, g is the gravitational acceleration, $\ddot{s}$ is the acceleration of the sphere, W is the weight of the sphere in air, B is buoyant force, D is the drag force on the sphere, K is the virtual mass coefficient of the sphere, ρ is the density of water, and V is the volume of the sphere. The moment of inertia and frictional torque of the pulley have been neglected. Solving Eq. 4 for T, and substituting into Eq. 5 gives

$$\left(\frac{W}{g} + \frac{w}{g} + K\rho V\right)\ddot{s} = W - w - B - \underline{C}\ \tfrac{1}{2}\rho A \dot{s}^2 \tag{6}$$

where $\underline{C} = \dfrac{D}{\frac{1}{2}\rho A \dot{s}^2}$, which is a function of time due to the non-constant velocity $\dot{s}$, and is therfore not a correct expression for the terminal coefficient of drag. For st4ady state conditions, $\ddot{s}$ is zero and $\dot{s}$ equals the terminal velocity, v,

$$v = \left(\frac{W - w - B}{C_D\ \frac{1}{2}\rho A}\right)^{1/2} \tag{7}$$

where C_D is the terminal drag coefficient.

For convenience, define a parameter a, which equals

$$a = \frac{\left[(W - w - B)(C_D\ \frac{1}{2}\rho A)\right]^{1/2}}{\left(\frac{W+w}{g} + K\rho V\right)} \tag{8}$$

where C_D is the actual coefficient of drag for the sphere at terminal velocity. With rearrangement, Eq. 6 becomes

$$\ddot{s} = a\left(v - \frac{\underline{C}}{C_D}\frac{\dot{s}^2}{v}\right) \tag{9}$$

In order to proceed further, it is necessary to assume that K is constant and that $\underline{C} = C_D$. It is then possible to integrate Eq. 9, which becomes

$$\dot{s} = v \tanh(at) \tag{10}$$

and a second integration gives

$$s = \frac{v}{a} \ln[\cosh(at)] \tag{11}$$

where s is the fall distance. By setting the velocity s equal to 0.99v, the tanh(at) equals 0.99 from Eq. 10 and the ln[cosh(at)] equals 1.96 from Eq. 11. The distance required to reach 0.99 terminal velocity is then given by

$$s(.99) = 1.96\, v/a \tag{12}$$

Substitution of Eqs. 7 and 8 into Eq. 12 gives

$$s(.99) = \frac{1.96m\left(\frac{W+w}{\rho g v} + K\right)}{\frac{1}{2}\rho A C_D} = \frac{1.96\, m\left(\rho'/\rho + K\right)}{\frac{1}{2}\rho A C_D} \tag{3}$$

where m is the water mass displaced by the sphere and $\rho' = \frac{W+w}{gv}$

At this point, the acceleration factor α, is introduced and defined as the ratio of measured velocity $\dot{s}$, to terminal velocity v. By use of this ratio and letting t_α be the time when $\dot{s} = \alpha v$, Eq. 10 becomes

$$at_\alpha = \tanh^{-1}\alpha = \frac{1}{2}\ln\frac{1+\alpha}{1-\alpha} \tag{13}$$

and

$$s(\alpha) = \frac{m(\rho'/\rho + K)}{C_D \frac{1}{2}\rho A} \ln[\cosh(at_\alpha)] \tag{14}$$

If $s(\alpha)$ is set equal to the actual fall distance, Eq. 14 can be solved for $\cosh(at_\alpha)$ to give

$$\cosh(at_\alpha) = e^{\frac{h C_D}{b}} \tag{15}$$

where

$$b = \frac{m(\rho'/\rho + K)}{1/2\, \rho A} .$$

The left hand side of Eq. 15 can be rewritten in exponential form and use can be made of Eq. 13 to give

$$\cosh(at_\alpha) = \frac{1}{2}\left(e^{at_\alpha} + e^{-at_\alpha}\right)$$

$$= \frac{1}{2}\left(e^{\ln\left(\frac{1+\alpha}{1-\alpha}\right)^{1/2}} + e^{-\ln\left(\frac{1+\alpha}{1-\alpha}\right)^{1/2}}\right) \tag{16}$$

Equations 15 and 16 can be equated to eliminate $\cosh(at_\alpha)$, and the relation between C_D and α becomes

$$\left[\left(\frac{1+\alpha}{1-\alpha}\right)^{1/2} + \left(\frac{1-\alpha}{1+\alpha}\right)^{1/2}\right] = 2e^{\frac{h C_D}{b}} \tag{17}$$

which, when simplified and solved for α^2, gives

$$\alpha^2 = 1 - e^{-\frac{2h C_D}{b}} \tag{18}$$

In this equation, C_D is the coefficient of drag for a body at terminal velocity. By definition of α, C_D is

$$C_D = \frac{\text{Drag Force}}{1/2\, \rho A v^2} = \frac{W - w - B}{1/2\, \rho A \dot{s}^2}\, \alpha^2 \tag{19}$$

Therefore,

$$C_D = \alpha^2 C \tag{20}$$

where C is the measured coefficient of drag using the terminal drag (W-w-B) and the instantaneous velocity $\dot{s}$. Equation 18 then becomes

$$1-\alpha^2 = e^{-\frac{2h}{b}\alpha^2 C} \tag{21}$$

In order to apply Eq. 21, it is convenient to plot $\frac{2h}{b}C$ versus α^2, with α^2 as a variable. Then by computing the quantity $\frac{2h}{b}C$ for each drop, the α^2 correction can be taken from the graph and Eq. 20 applied to obtain the corrected coefficient of drag.

The virtual mass coefficient K appears as a factor in b, and is an important factor in the calculations. Although K is not known accurately, theoretical estimates for K are given as .5 for a sphere with turbulent boundary layer separation and 1.8 for a sphere with laminar separation [4]. These values of K were used in applying equation 21 for the determination of α^2, and the validity of the above estimates is discussed in the Results section.

The approximation that $\underline{C} = C_D$ is valid only where the drag curve is essentially horizontal. In the critical Reynolds number region, this approximation is no longer valid, but it is hoped that this procedure will still give an indication of the existence of a critical Reynolds number. Beyond the critical Reynolds number, the value of the drag coefficient is not to be relied upon.

Since Reynolds number is defined in terms of the terminal velocity, the α correction is applied as follows:

$$\text{Re(corrected)} = \frac{vd}{\nu} = \frac{\dot{s}d}{\alpha\nu} = \frac{\text{Re(measured)}}{\alpha} \tag{22}$$

6. Results

6.1 Water. In order to determine the capabilities and accuracy of the experimental technique, a series of tests in water were made prior to making any drops in polymer solutions. It was determined from these tests that investigations could be conducted in the Reynolds number region of 4×10^4 to 4×10^5. The results of the water drops are shown in Fig. 6, with two additional curves plotted for reference. The lower curve is the classical drag curve plotted from data taken in water and air, with wind tunnel results used for the critical Reynolds number region and above [7]. The top curve is plotted from free fall of a sphere in air, as reported by Lunnon [8], and by Bacon and Reid [9]. Rotation of the sphere during the drop is Goldstein's [10] possible explanation for the difference between wind tunnel results and free-fall results.

Since the tank was determined to be of insufficient depth for attainment of terminal velocity at the higher speeds investigated, acceleration correction factors were applied to all data points, as shown in Fig. 7.

In correcting the data points, two different values of the virtual mass coefficient K were used, 0.5 and 1.8. The value K=0.5 is the theoretical value obtained for an inviscid fluid, and is assumed to be applicable to flow in the supercritical region. In the subcritical region there is no substantiated value of K, but following Lang and Patrick [4], K=1.8 was used. This provided for analysis of the effect of K in both the subcritical and supercritical regions. The results show that the value of K=1.8 produces a curve which is in excellent agreement for Reynolds numbers less than 1.3×10^5, but falls off rapidly above this value. The value of K=0.5 produces a better fit for Reynolds numbers above 1.3×10^5. Due to the assumption concerning the equality of drag coefficients ($\underline{C}=C_D$), it was impossible from this experiment to comment further on the validity of this value of K=0.5 for the supercritical region.

The dashed line in Fig. 7 is a fit to the corrected data points and is in excellent agreement with the classical drag curve in the subcritical region. However, the correction factors produced a curve which decreased only gradually near the critical Reynolds number. This was due to the assumption in the correction calculations that $\underline{C}$, the time dependent drag coefficient, is equal to C_D, the terminal drag coefficient. This assumption was necessary to solve the equation of motion, but is valid only where the drag curve is essentially horizontal. As a result, all data points in the turbulent region are good approximations only, and should not be considered entirely accurate. The value of these data points is in the fact that they do show the qualitative behavior of a sphere in the supercritical region.

Pulley friction was measured in a separate air drop test and a friction drag correction was computed for all velocity ranges. This correction factor was smaller by a factor of 10^{-3} than any measured drag coefficients and therefore, was not applied to any values.

6.2 Polymer Solutions. Drag reduction for spheres falling in a high polymer solution was investigated for five different concentrations of WSR 301: 50, 100, 200, 500, and 1000 wppm. The results of these investigations are shown in Fig. 8 for 100 wppm and Fig. 9 for 1000 wppm solutions, with both uncorrected and corrected data points shown. In making the acceleration corrections, it was assumed that the two values of K are the same as for water. Note that the Reynolds numbers where the value of K is changed are about the same as for water. Only representative corrected points are shown, but all original data is plotted to show the continuity of results. Results were obtained for the subcritical and the supercritical regions for all concentrations. Excellent correlation with previous results obtained in the subcritical region can be noted.

In the subcritical region, all concentrations exhibited a high degree of drag reduction, with the 100 wppm solution being the most efficient below a Reynolds number of 10^5. Above a Reynolds number of

10^5, the 1000 wppm solution becomes the more effective drag reducer. This effect was also observed by Lang and Patrick [4]. Above a Reynolds number of 10^4, the 100 wppm solution produced a drag curve similar in shape to that of water, in that the curve continues almost horizontally until a sharp drop-off, which occurs at a critical Reynolds number somewhat beyond that of water. In contrast, the drag curve produced by the 1000 wppm solution decreased uniformly without the sharp drop-off associated with water and 100 wppm polyox.

The uncorrected results for all concentrations are plotted in Fig. 10. From this figure, it was noted that the 50 and 100 wppm solutions exhibited like behavior, while the 200 and 500 wppm solutions have drag curves similar to that of the 1000 wppm solutions.

Since a non-mechanical method of mixing was employed, a time degradation study was conducted with the 100 wppm solution. The results are shown in Fig. 11 and indicated a gradual increase in drag over a period of 8 days, which was the limit of the test.

7. Conclusions

The behavior of blunt bodies in high polymer solutions is dependent upon polymer concentration and Reynolds number. For the Reynolds number range up to 10^5, the amount of drag reduction in dilute polymer solutions (100 wppm and less) increases with velocity. The shape of the drag curve above 10^5 is similar to that of water, with the transition to turbulent flow occurring at a Reynolds number of about 4.5×10^5.

For more concentrated solutions (200 wppm and above), the amount of drag reduction observed increases continuously up to a Reynolds number of 5×10^5, the upper limit of study. A critical Reynolds number does not seem to exist.

In an attempt to explain the shape of the curves described above, the effect of polymer concentration upon the wake diameter of blunt bodies will be explained in three different Reynolds number ranges as shown in Fig. 12. Region 1 extends from 4×10^3 to 10^4, region 2 from 10^4 to 10^5, and region 3 from 10^5 to 6×10^5. In addition to the classical drag curve for water, curves for the 100 wppm and 1000 wppm concentrations of polymer solutions were drawn from data taken during this experiment, combined with data obtained by Ruszczycky [1], Lang and Patrick [4], and Hayes [2].

If the primary effect of polymer additives in water is to decrease the wake diameter of blunt bodies by moving the separation point rearward, thereby stabilizing the laminar boundary layer and thus decreasing drag, the following mechanism can be postulated:

(A) Dilute concentrations (100 wppm and less)

1. There is no drag reduction in region 1 due to the fact that the increase in friction drag overwhelms any decrease in profile drag.

2. In region 2, friction drag becomes negligible at a Reynolds number of 10^4 and profile drag predominates as velocity increases. Drag reduction occurs because the wake diameter is decreased by the polymer additive.

3. Drag reduction is still apparent in region 3 until the critical Reynolds number for water is reached. Since the polymer additives have decreased the wake diameter by stabilizing the laminar boundary layer, turbulent separation is delayed beyond that of water, but not prevented as can be seen from the sudden drop-off at a Reynolds number of 4.5×10^5.

(B) Concentrated solutions (200 wppm and above)

1. Again there is no drag reduction in region 1 for the same reason as above.

2. In region 2, the friction drag associated with the higher concentrations postpones the onset of drag reduction until Reynolds number equals 1.5×10^4. Above this point, the amount of drag reduction increases almost continuously. In comparison to dilute solutions, the amount of drag reduction is less because of the higher friction associated with the higher concentrations.

3. The drag curve continues to decrease uniformly in region 3. This is probably due to the fact that the higher concentrations are able to produce a smaller wake. The concentrated solutions are the more effective drag reducers in region 3. Due to the small wake, any transition to turbulent flow will be unobservable.

4. All solutions of concentration 200 wppm and above produce the same results in the critical Reynolds number region, indicating a saturation effect.

In addition to the above conclusions, it was noted that non-mechanical mixing decreases the rate of time degradation of polymer solutions.

ACKNOWLEDGMENT

The author wishes to thank Professor J. V. Sanders for his many helpful suggestions and for the hours of assistance spent in assuring the successful completion of this research.

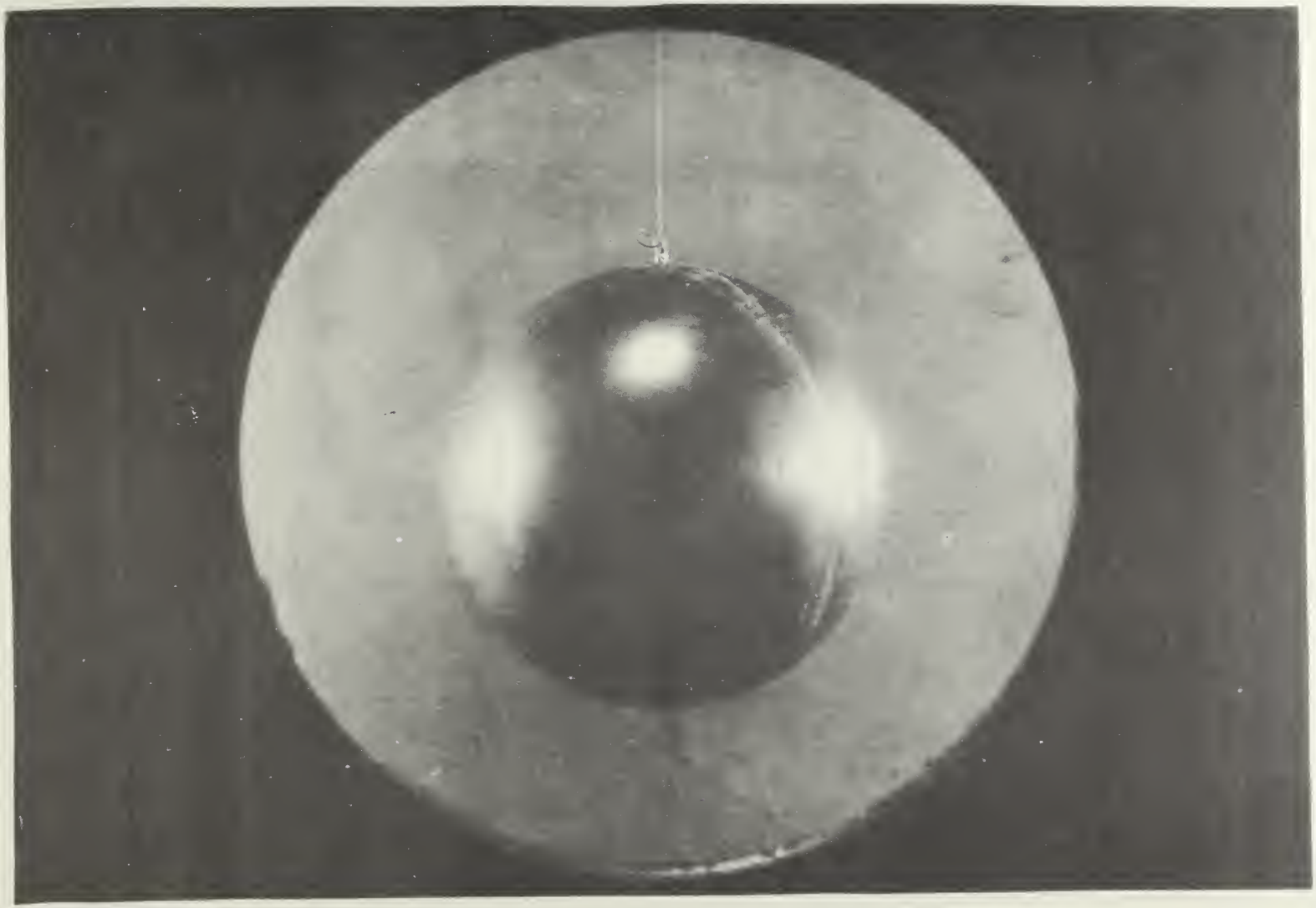

Figure 1. Porthole view of sphere in polymer solution.

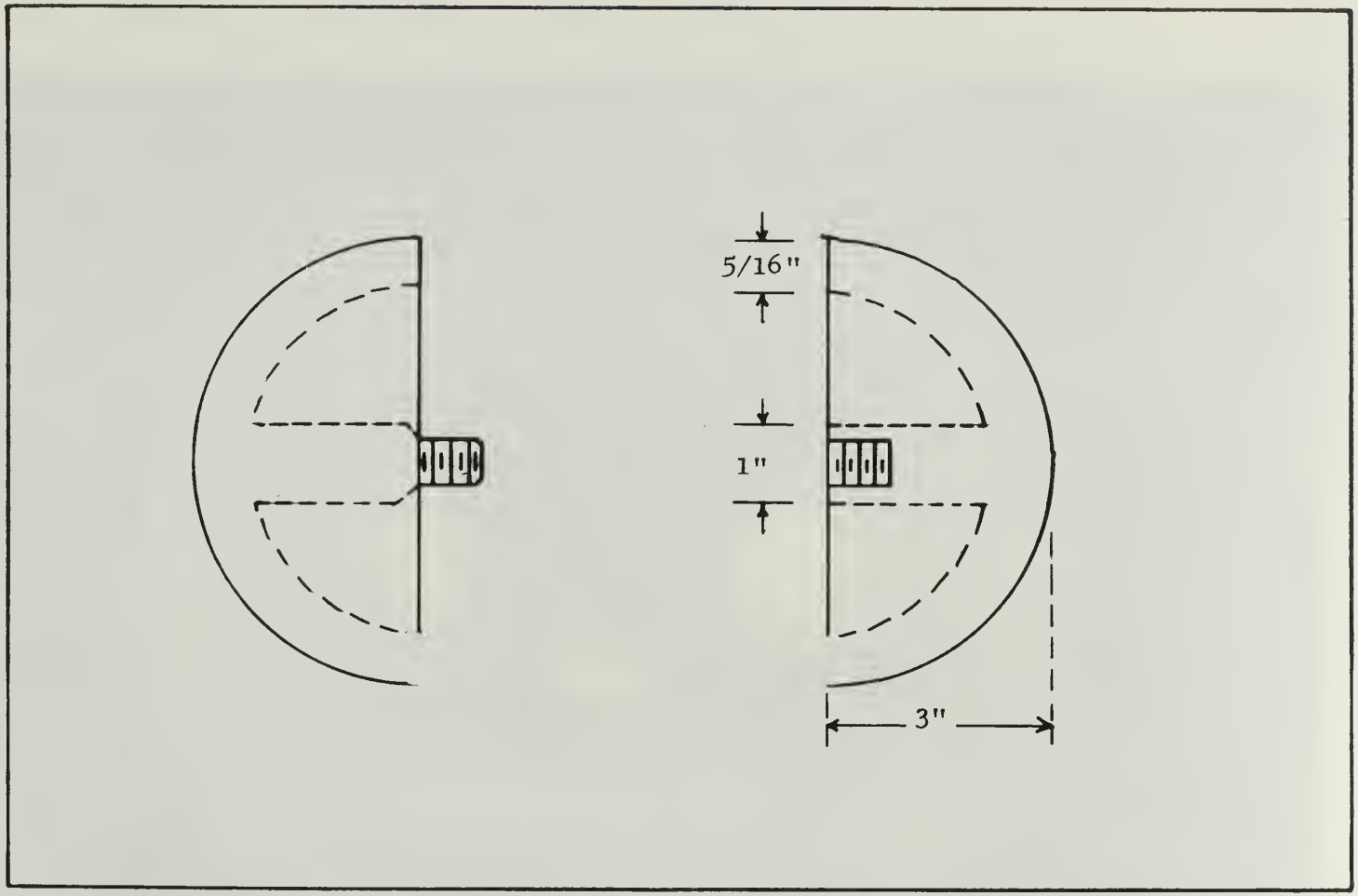

Figure 2. Separated view of test sphere.

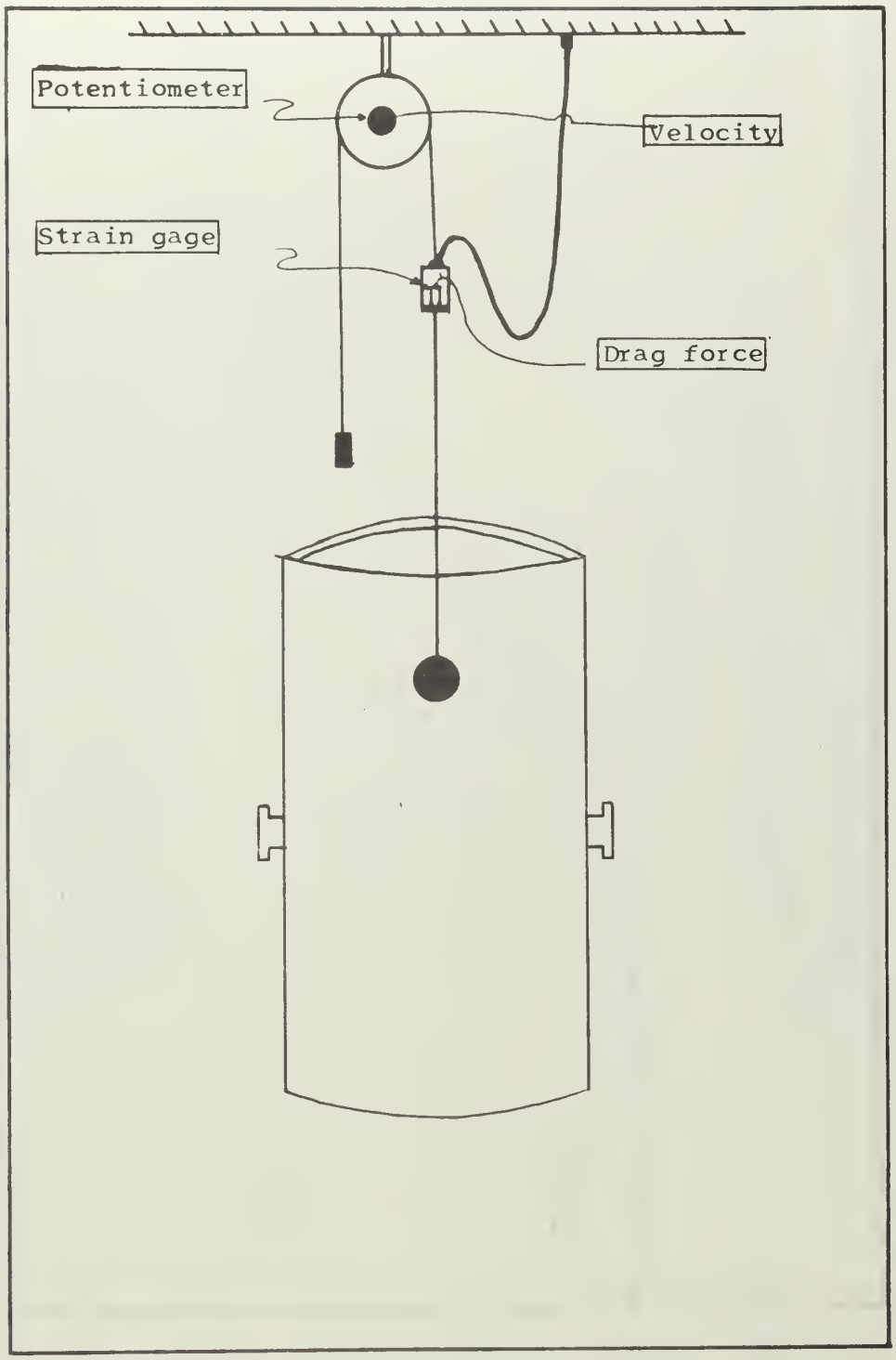

Figure 3. Experimental drop mechanism.

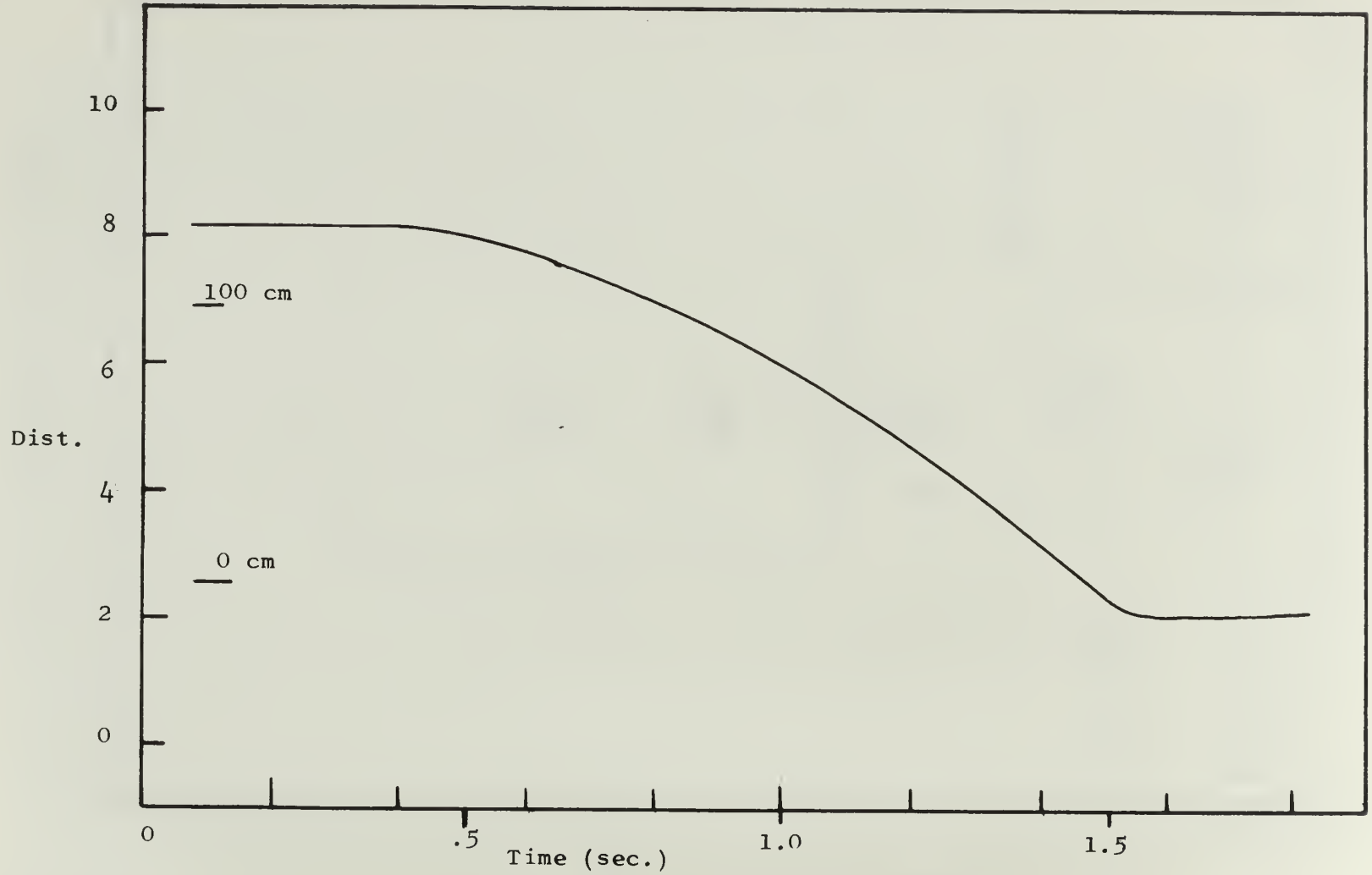

Figure 4. Typical potentiometer output.

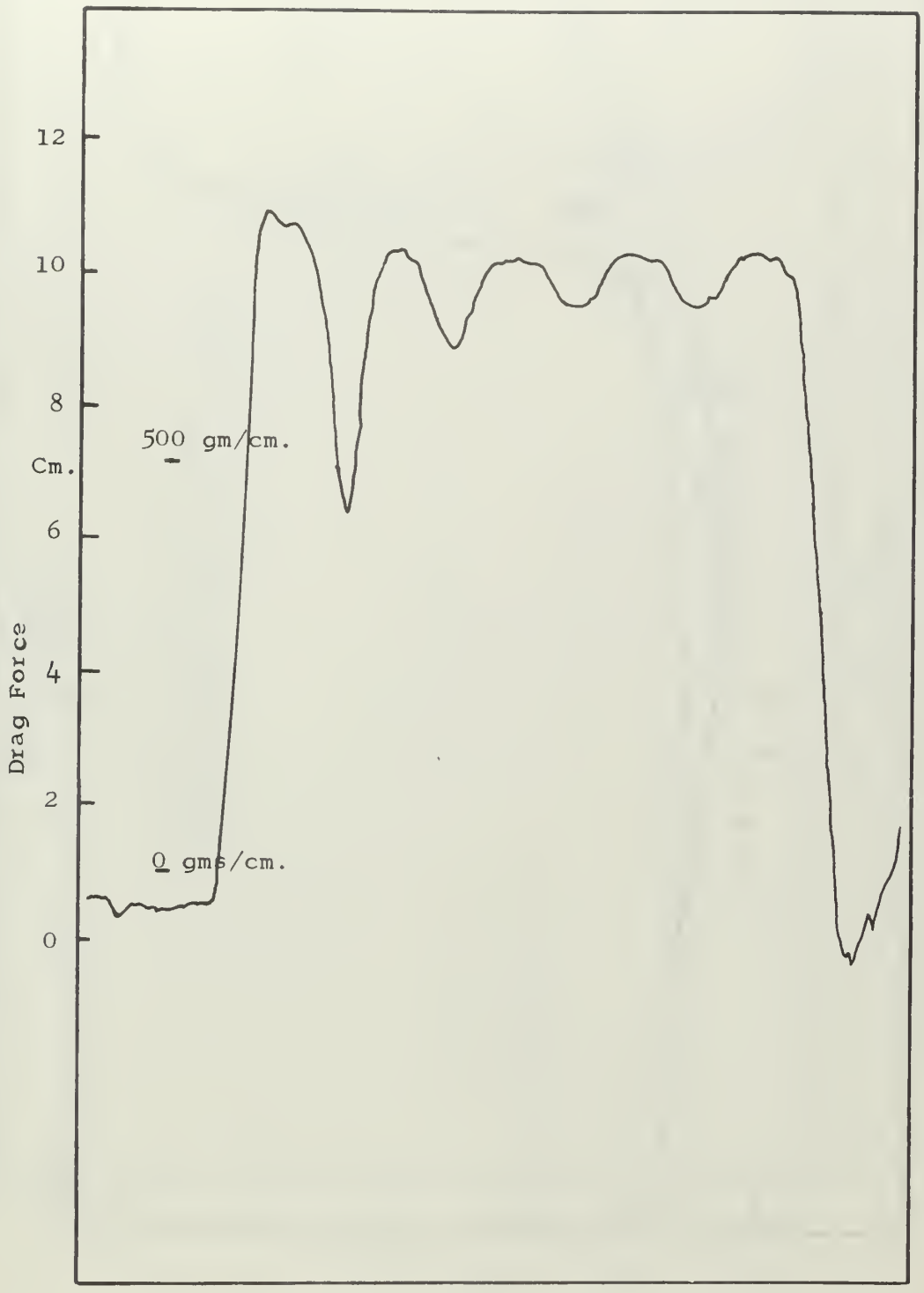

Figure 5. Typical strain gage output.

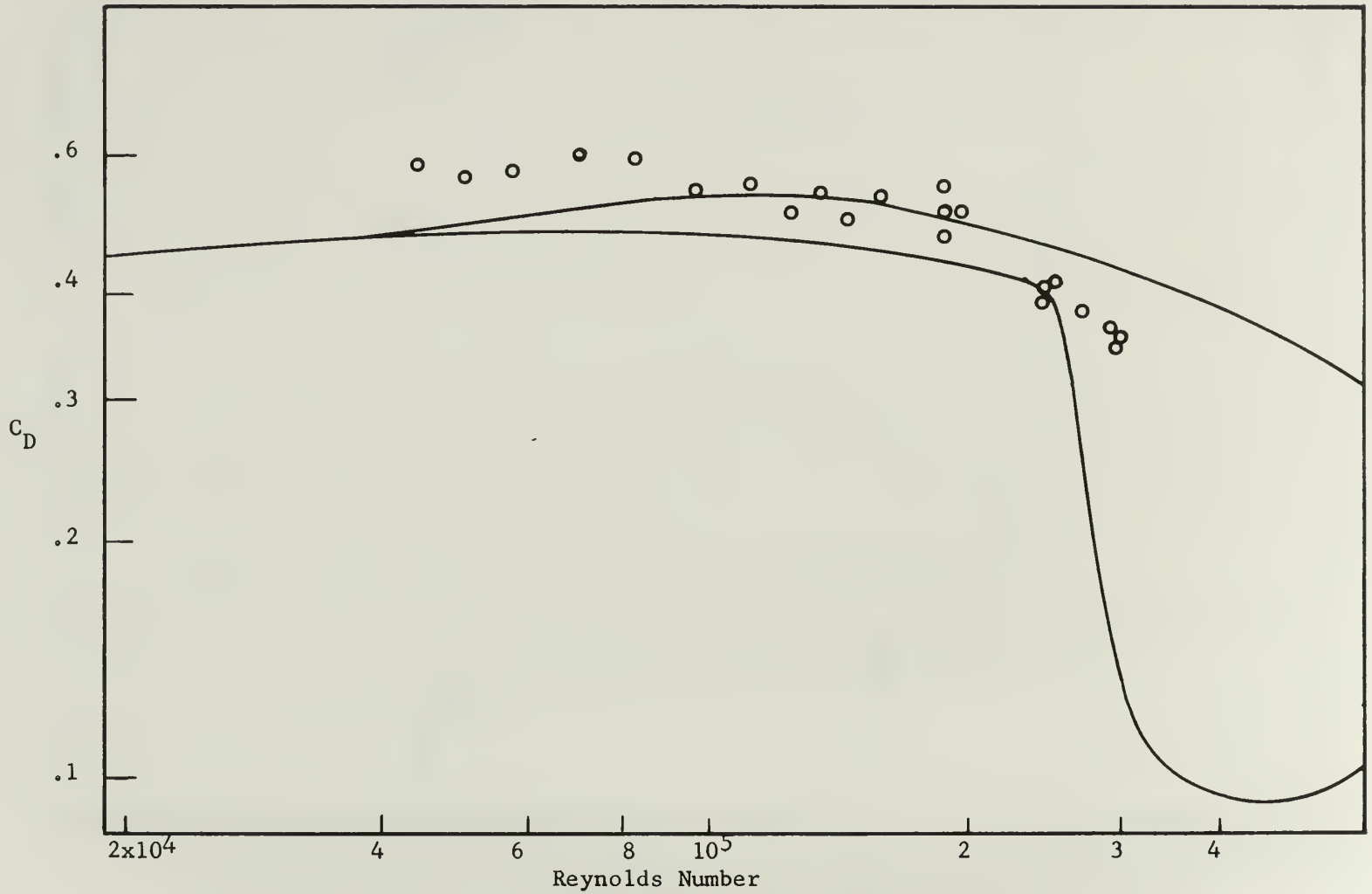

Figure 6. Drag coefficients for a six inch sphere in water. (no acceleration correction)

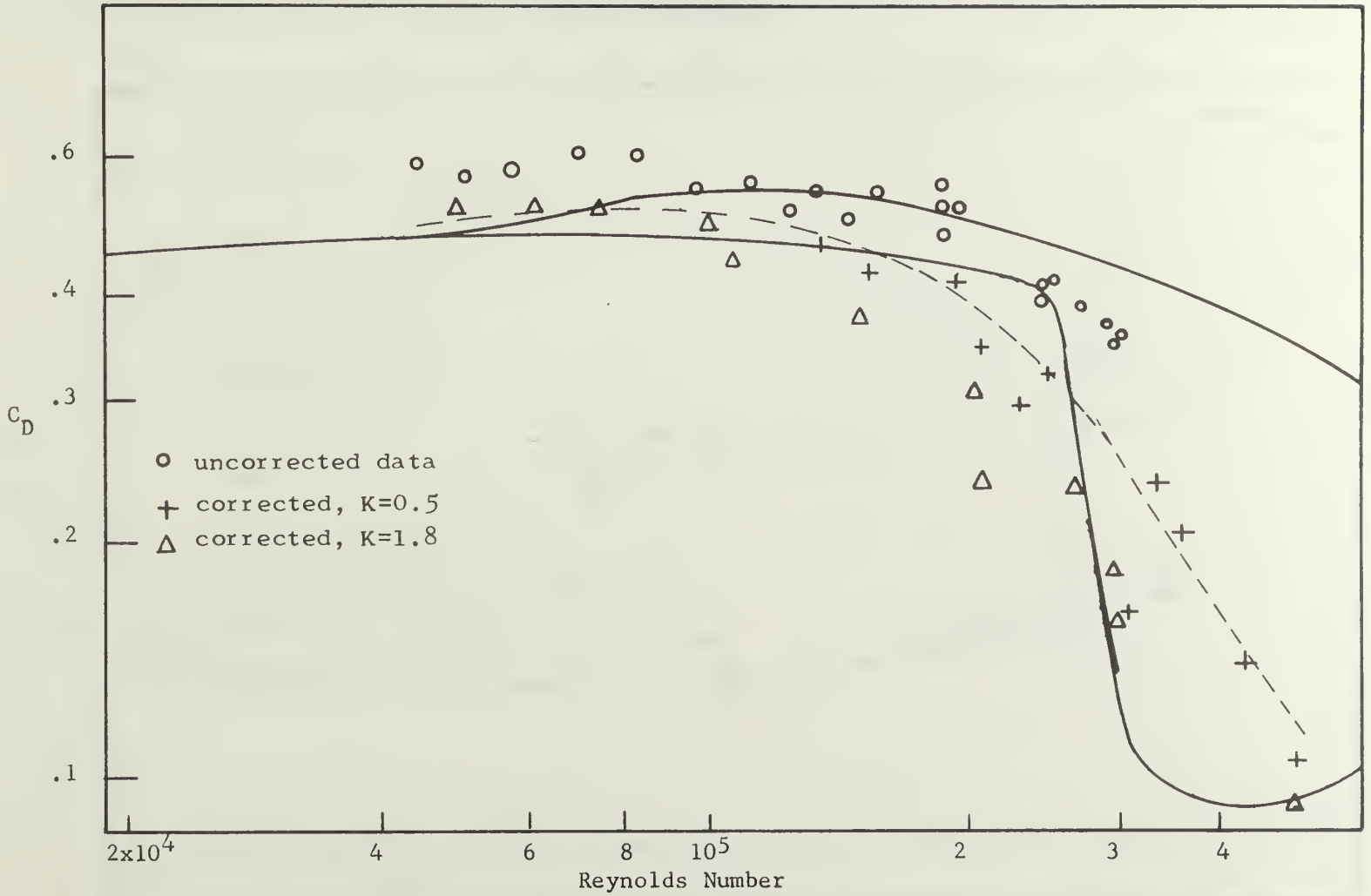

Figure 7. Drag coefficients for a six inch sphere in water. (acceleration corrected)

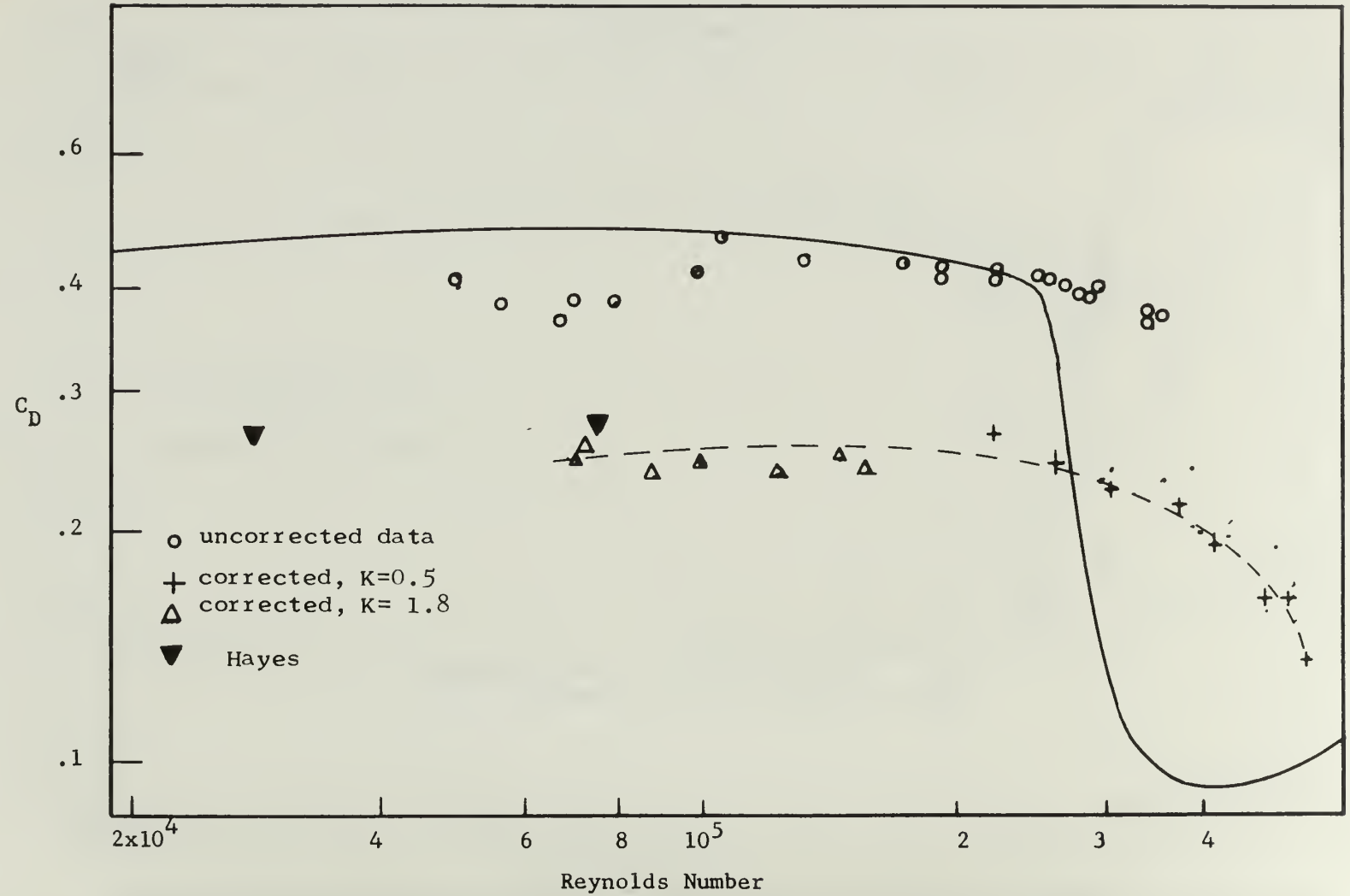

Figure 8. Drag coefficients for a six inch sphere in 100 wppm, WSR 301.

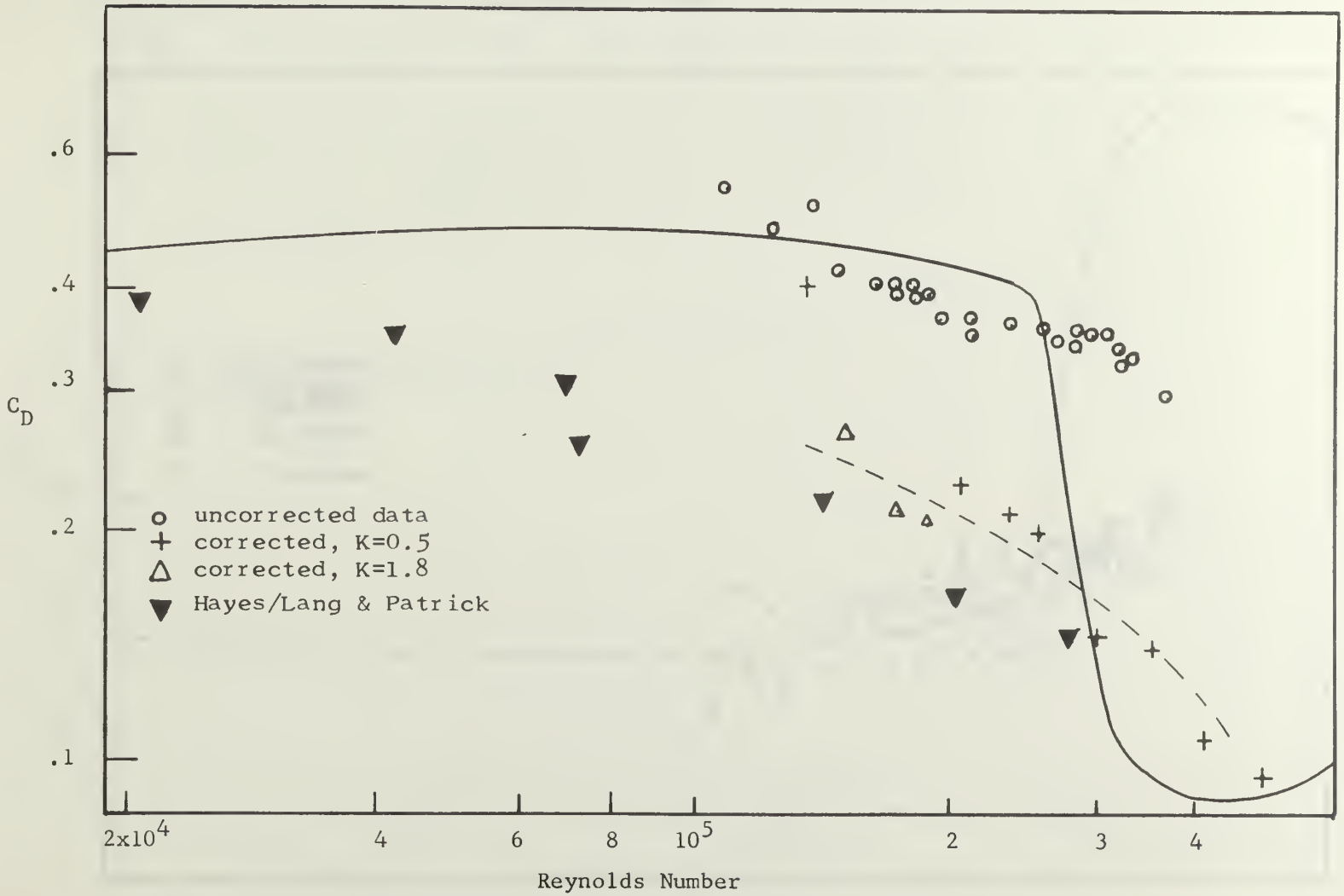

Figure 9. Drag coefficients for a six inch sphere in 1000 wppm, WSR 301.

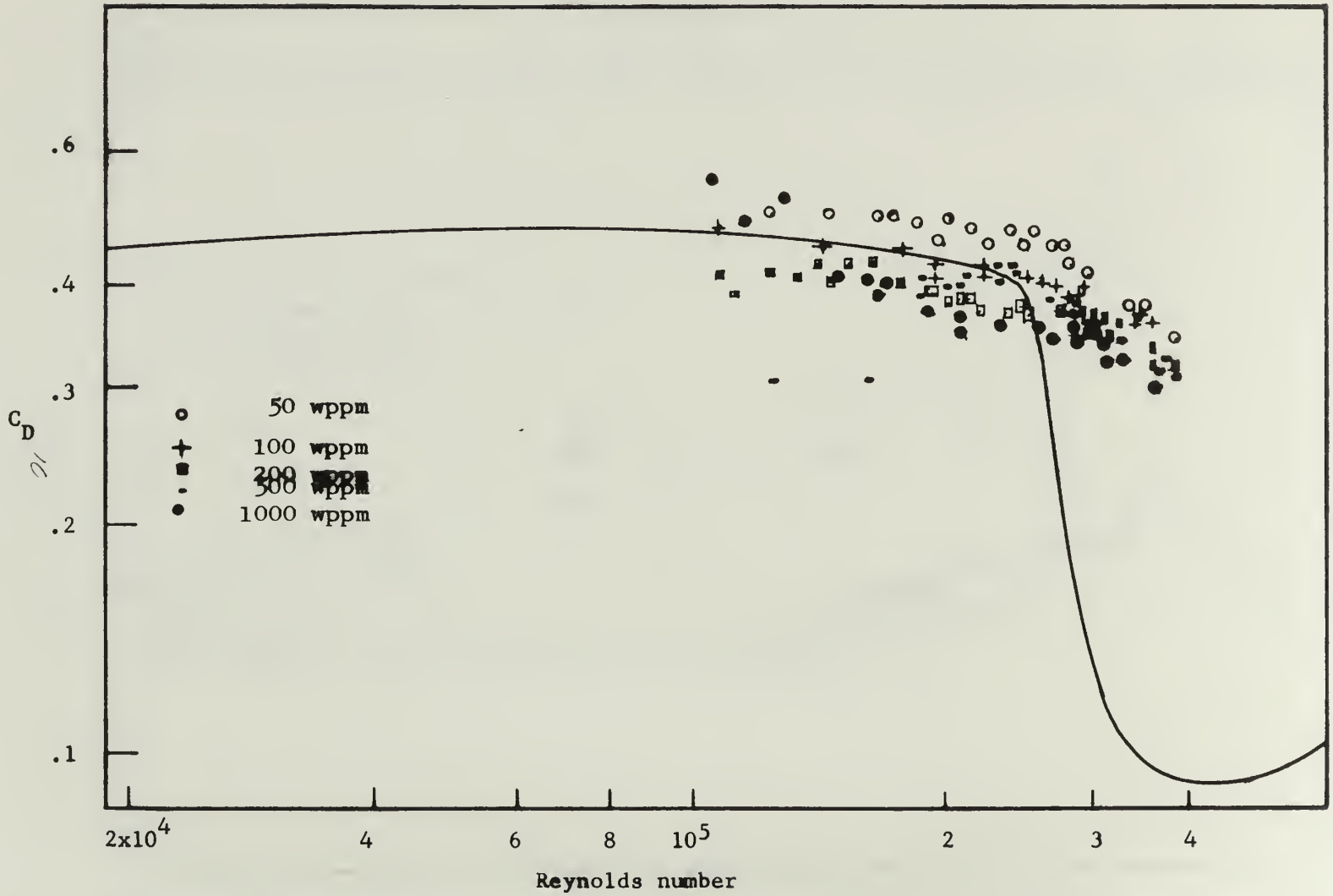

Figure 10. Drag coefficients for a six inch sphere in various concentrations of WSR 301. (no acceleration correction)

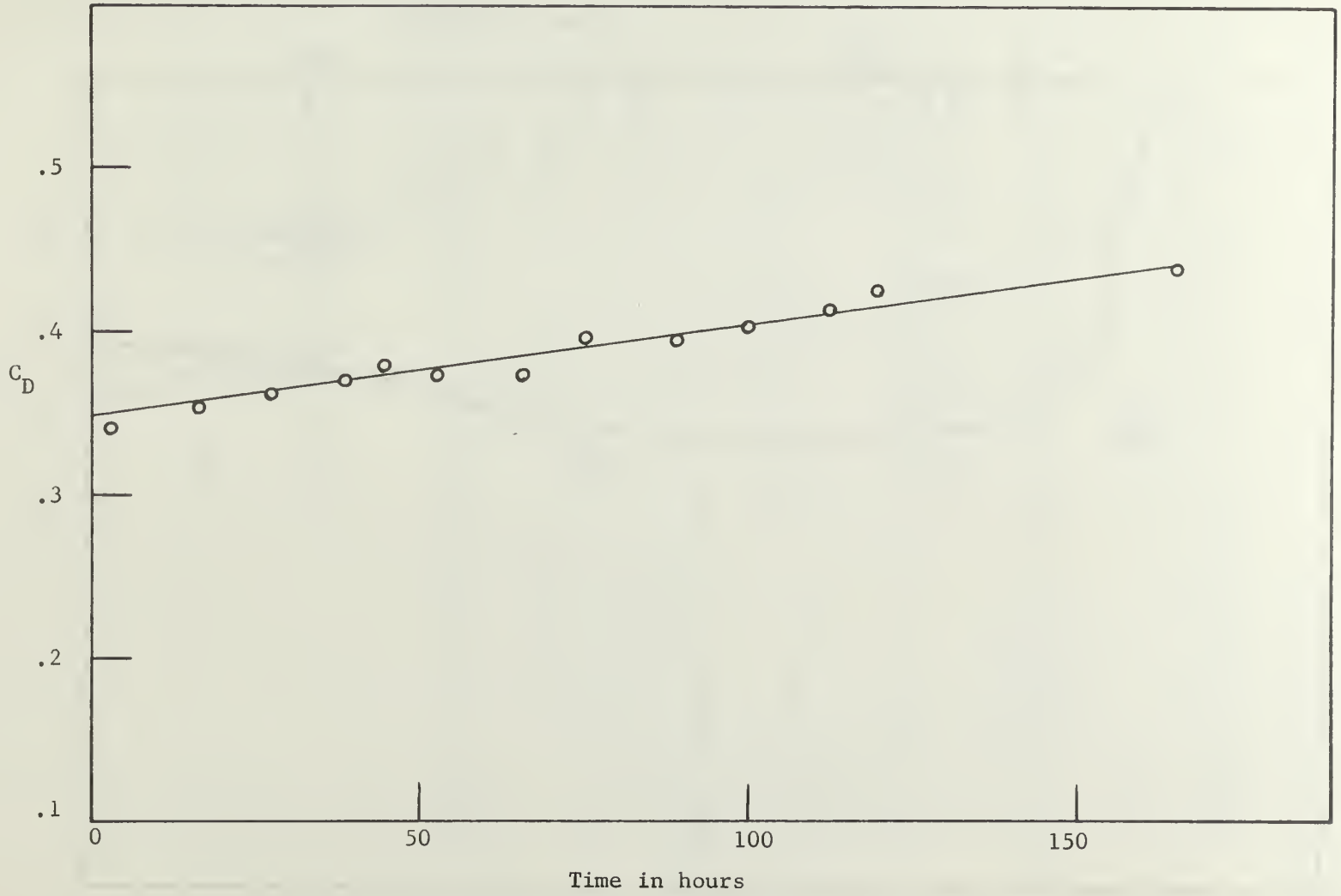

Figure 11. Ageing test for 100 wppm, WSR 301.

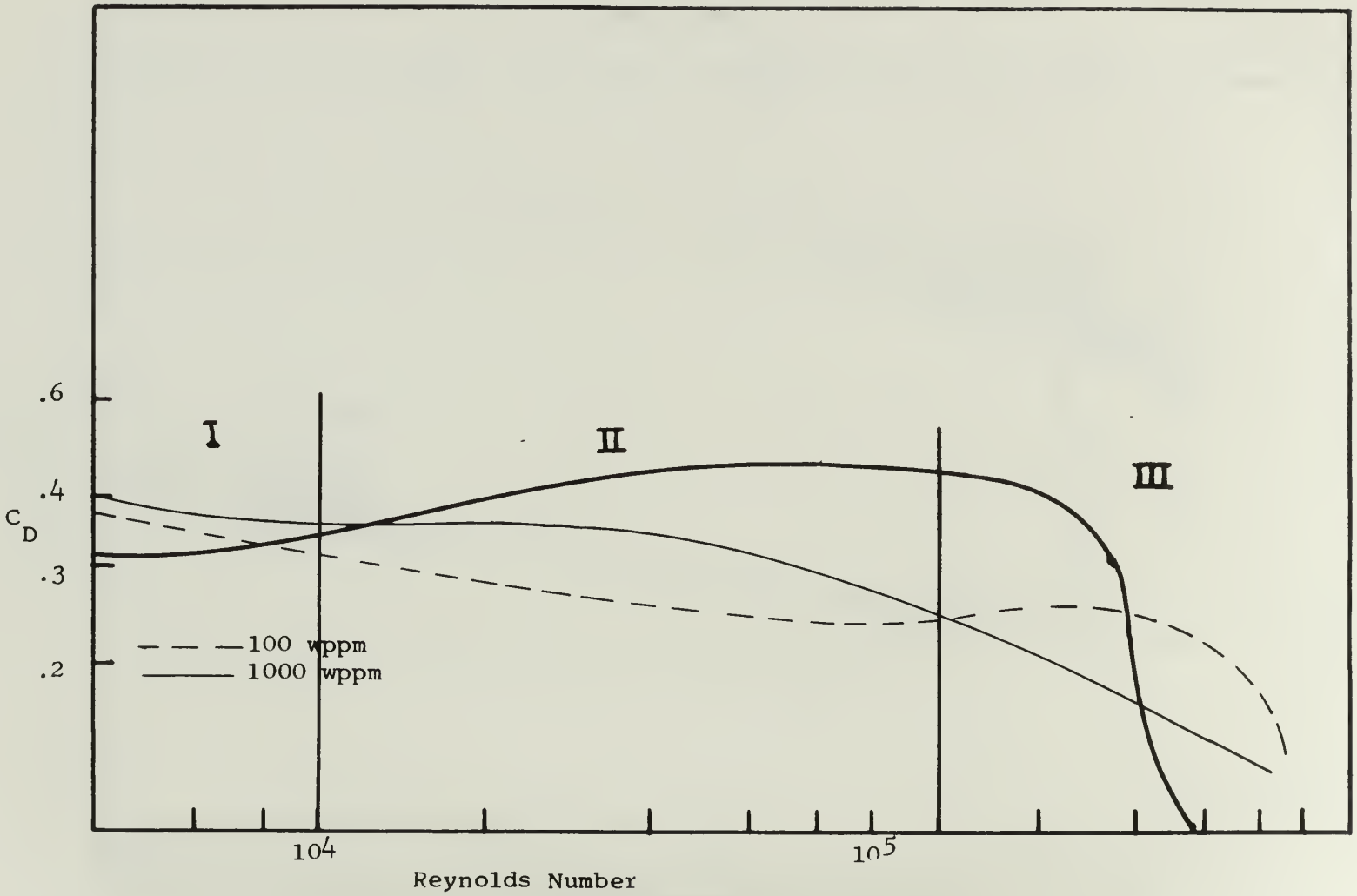

Figure 12. Drag coefficients for spheres in water, 100 and 1000 wppm WSR 301, combined results.

BIBLIOGRAPHY

1. M. A. Ruszczycky, "Sphere Drop Tests in High Polymer Solutions," Nature, 206, 614, (1965).

2. M.F. Hayes, "Drag Coefficients of Spheres Falling in Dilute Aqueous Solutions of Long-Chain Macromolecules," Thesis, Naval Postgraduate School, Monterey, Calif., (1966).

3. D.A. White, Nature, 212, 227, (1966).

4. T.G. Lang and H.V.L. Patrick, "Drag of Blunt Bodies in Polymer Solutions," Naval Ordnance Test Station TP 3670, (1967).

5. A. White, Nature, 211, 390, (1966).

6. J.W. Hoyt and A.G. Fabula, Naval Ordnance Test Station TP 3670, (1964).

7. H. Schlichting, "Boundary Layer Theory," (McGraw-Hill Book Co., Inc., New York, 1960), 4th ed.

8. R.G. Lunnon, Proc. Roy. Soc. (London), 118, 680-694, (1928).

9. D.L. Bacon and E.G. Reid, N.A.C.A. Report #185, (1924).

10. S. Goldstein, "Modern Developments on Fluid Dynamics," (Dover Publications, Inc., New York, 1965), Vol II.

11. J. Levy and S. Davis, "Drag Measurements On a Thin Plate in Dilute Polymer Solutions," International Shipbuilding Progress, 14, 166, (1967).

INITIAL DISTRIBUTION LIST

		No. Copies
1.	Defense Documentation Center Cameron Station Alexandria, Virginia 22314	20
2.	Library Naval Postgraduate School Monterey, California 93940	2
3.	Naval Ship Systems Command Navy Department Washington, D.C.	1
4.	Prof. James V. Sanders Department of Physics Naval Postgraduate School Monterey, California 93940	10
5.	LT John H. Chenard 7 Sherbrooke Ave. Lewiston, Maine	2

DOCUMENT CONTROL DATA - R&D

(Security classification of title, body of abstract and indexing annotation must be entered when the overall report is classified)

1. ORIGINATING ACTIVITY *(Corporate author)*

Naval Postgraduate School
Monterey, California 93940

2a. REPORT SECURITY CLASSIFICATION
Unclassified

2b. GROUP

3. REPORT TITLE

Drag of Spheres in Dilute Aqueous Solutions of Poly(ethylene oxide) Within the Region of the Critical Reynolds Number

4. DESCRIPTIVE NOTES *(Type of report and inclusive dates)*
Masters thesis - December 1967

5. AUTHOR(S) *(Last name, first name, initial)*

Chenard, John H. Lieutenant United States Navy

6. REPORT DATE	7a. TOTAL NO. OF PAGES	7b. NO. OF REFS
December 1967	44	11

8a. CONTRACT OR GRANT NO.	9a. ORIGINATOR'S REPORT NUMBER(S)
b. PROJECT NO.	
c.	9b. OTHER REPORT NO(S) *(Any other numbers that may be assigned this report)*
d.	

10. AVAILABILITY/LIMITATION NOTICES [redacted]

11. SUPPLEMENTARY NOTES

12. SPONSORING MILITARY ACTIVITY

This document has been approved for public release and sale; its distribution is unlimited.

1/15/71

13. ABSTRACT

The drag reducing effect of poly(ethylene oxide) additives on blunt bodies in water was investigated by examining the behavior of a sphere in both subcritical and supercritical Reynolds number regions. Drop tests were conducted in water and in concentrations of poly(ethylene oxide) WSR 301 ranging in concentration from 50 wppm to 1000 wppm. Reduction in drag was noted for all concentrations in the Reynolds number range of 4×10^4 to 3.5×10^5. A critical Reynolds number of 4.5×10^5 was observed for dilute solutions (50 and 100 wppm), while more concentrated solutions exhibited a uniformly decreasing drag. These results are explained by examining the interaction of profile and friction drag, together with the effects of polymer additives upon wake diameter size.

DD FORM 1 JAN 64 1473

14. KEY WORDS	LINK A		LINK B		LINK C	
	ROLE	WT	ROLE	WT	ROLE	WT
Drag reduction						
Poly(ethylene oxide)						
Blunt bodies						
Critical Reynolds number